

Development of Computational Approaches Towards a Proposal of Quantitative Biomarker Using LiTS and CHAOS Data for Hepatic Neoplasms.

J. Ricardo Hernandez¹, Dagoberto Armenta-Medina² and Guillermo Ruiz¹

¹Centro de Investigación e Innovación en Tecnologías de la Información y Comunicación (INFOTEC), Aguascalientes 20326, México

²Consejo Nacional de Ciencia y Tecnología (CONACyT), Ciudad de México 03940, México.

Abstract

This study focuses on analyzing tomographic images from the LiTS (Liver Tumor Segmentation Challenge) and CHAOS (Combined CT-MR Healthy Abdominal Organ Segmentation) datasets, comprising 40 patients, half with hepatic neoplasms (LiTS) and the rest healthy liver donors (CHAOS). The primary aim is to employ fractal dimension as a tool for characterizing hepatic organ morphology. The first step of analysis is a preprocessing 11,311 images, with a technique of pixel intensity weighting for effective liver segmentation. Binary classification categorized pixels, indirectly capturing organ contrast distribution. This preprocessing enriched subsequent fractal dimension analysis.

Original images underwent pixel scanning and mean calculation for thresholding, this for transforming them into binary images. The calculation of the fractal dimension followed, the images with black pixels were filtered, resulting in 3,412 pathological images and 2,289 non-pathological images.

Statistical analysis revealed a significant difference in fractal dimension between patient groups ($p: 4.965e-39$), indicating varying liver morphology in the groups. A box plot visually represented fractal dimension density, highlighting lower values for patients with hepatic pathologies (mean = 1.25) compared to those without (mean = 1.36).

Additionally, a comprehensive database of images was compiled. This database includes the medical images with the segmented liver as well as their original versions. To facilitate future research and contribute to diagnosis and classification of hepatic diseases, this database will be made available online to the scientific community.

Keywords

Image Analysis, Fractal Dimension, Segmentation, Box counting, Neoplasia

1. Introduction.

According to the World Health Organization (WHO), cancer stands as the second leading cause of mortality worldwide. In 2015 alone, this devastating disease claimed the lives of 8.8 million individuals, with liver cancer alone accounting for 788 thousand deaths. Many of these fatalities can be attributed to the lack of timely diagnosis and treatment, resulting in the detection of tumors at advanced stages. Consequently, there exists a pressing need to identify novel techniques founded on biomarkers to aid in early detection of this condition. Such biomarkers not only encompass clinical blood chemistry analysis but also encompass the incorporation of liver lesion images that manifest during the initial stages of the disease [1].

In addition to the profound loss of human life, cancer also exacts a considerable toll on global economies. Estimations reveal that the total cost associated with cancer in 2010 amounted to a staggering \$1.16 trillion. Disturbingly, as of 2017, merely 26% of low-income countries reported


CISETC 2023: International Congress on Education and Technology in Sciences, December 04–06, 2023, Zacatecas, Mexico

✉ jrhernandezm@outlook.com (J. Hernández-Morales); dagoberto.armenta@infotec.mx (D. Armenta-Medina); memoruiz@gmail.com (G. Ruiz-Velázquez)

🆔 0009-0007-3364-0927 (J. Hernández-Morales); 0000-0002-7603-873X (D. Armenta-Medina); 0000-0001-7422-7011 (G. Ruiz-Velázquez)



© 2023 Copyright for this paper by its authors.
Use permitted under Creative Commons License Attribution 4.0 International (CC BY 4.0).

 CEUR Workshop Proceedings (CEUR-WS.org)

the provision of pathology services in their public health systems, which serve the general population. Comparatively, over 90% of high-income countries deliver cancer treatment services to their patients, with the corresponding figure dwindling to below 30% for low-income countries [2].

Given the dire implications of inadequate cancer care and management, researchers must address the ongoing research problem of developing innovative techniques rooted in the identification of biomarkers. It is imperative that these biomarkers enable prompt and accurate diagnosis, facilitating effective treatment strategies. Moreover, these biomarkers ought to extend beyond conventional clinical blood chemistry analysis, embracing the incorporation of liver lesion images that may manifest during the primary stages of the disease [3].

1.1 Liver Lesions.

The liver, a vital organ located in the right hypochondrium, stands out as the largest viscus within the human body. Given its position in the abdominal cavity, the liver plays essential roles in the regulation and maintenance of various metabolic and physiological processes. It is vital because it not only plays a crucial role in digestion and nutrient storage but also actively participates in detoxifying and filtering harmful substances. However, the significance of the liver is also marked by its susceptibility to a wide range of pathologies. These conditions can range from local disorders directly affecting the liver to systemic issues involving its function in conjunction with other organs and systems of the body. The diversity of liver diseases underscores the vulnerability and clinical importance of this organ in the context of human health [4]. Computed tomography is especially useful for the analysis and diagnosis of the organ. This imaging method provides a detailed and three-dimensional view of the liver, allowing for a meticulous exploration of its anatomical structure and the detection of potential alterations or pathologies. Being non-invasive, it emerges as an effective tool for evaluating liver morphology and function [5], in addition, it allows for extensive resolution and detailed reconstruction of the relevant area, as well as significant enhancement in the venous phase. In general, due to its moderate costs and almost guaranteed accessibility in our country, it is the primary study for liver evaluation. A hepatic lesion, also known as a focal lesion or space-occupying lesion, is characterized by being a presence within the complex hepatic parenchyma. This structure, which can manifest with a liquid or solid nature, is distinguished by its ability to displace surrounding formations, altering both the contour and, at times, the size of the liver [6], additionally, it is crucial to note that hepatic lesions, despite their presence in the organ, do not always lead to significant structural and functional alterations in the hepatic system. In many cases, these lesions may manifest as benign entities, meaning that, although they can be detected through imaging studies, they do not generate substantial adverse impacts on the integrity or functionality of the liver [7].

Within the spectrum of malignant lesions affecting the liver, Hepatocellular Carcinoma stands out as an entity of considerable clinical significance. This form of hepatic neoplasia ranks sixth globally in terms of frequency and represents the third leading cause of cancer-related mortality. In the Mexican context, a significant increase of 14% in mortality associated with this pathology was observed during the period between 2000 and 2006 [8], on the other hand, metastatic disease constitutes the most commonly found hepatic neoplasia in imaging studies [9].

1.2 Biomarkers and Cancer.

Human carcinogenesis, the process of cancer formation, is a complex phenomenon that initiates with a single cell and is characterized by uncontrolled cellular growth. This intricate process is a result of the interaction between external and internal factors, which provoke irreversible changes in cellular function. External agents, such as environmental carcinogens and radiation, intertwine with internal processes involving genetic and epigenetic alterations. This combination of factors triggers biochemical and molecular events that drive the transformation

of normal cells into cancerous ones, promoting unrestricted cell growth, which is a defining characteristic of malignant tumors. Understanding this molecular sequence is crucial for effectively addressing the development and progression of cancer [10].

The concentrations of carcinogens or their metabolites assessed in tissues or bodily fluids play a crucial role as indicators, known as cancer biomarkers. These biomarkers not only provide a direct window into exposure to carcinogenic substances but also serve as revealing signals of fundamental biological processes. Among these biological processes are xenobiotic metabolism, which addresses the transformation of foreign compounds in the body; DNA repair, which counteracts genetic damage; cell proliferation, which regulates cell growth; apoptosis, which controls programmed cell death; and the immune response, which plays a vital role in defense against abnormal cells. The comprehensive monitoring of these biomarkers provides a holistic view of exposure to carcinogens and associated biological responses, thus contributing to a more complete and accurate assessment of cancer risk [11] [12].

The significance of these biomarkers lies in their ability to provide early prognosis regarding the likelihood of developing cancer. This prognosis becomes an invaluable tool that enables medical professionals to make informed decisions about the initiation of specific treatments or appropriate interventions. By obtaining early information through the assessment of biomarkers, the door is opened to more proactive and personalized medical strategies, thus optimizing the effectiveness of therapeutic measures. Ultimately, the early identification of these cancer biomarkers not only enhances treatment prospects but can also be instrumental in prevention or early detection, significantly elevating the quality of healthcare provided to patients.

1.3 Fractal Dimension (FD).

In mathematics, the Hausdorff dimension is a measure of roughness first introduced in 1918 by the mathematician Félix Hausdorff. The Hausdorff dimension is an integer according to the usual sense of dimension, also known as topological dimension. Nevertheless, formulas have been developed to calculate the dimension of less simple objects, where, relying solely on their scale and self-similarity properties, it is concluded that objects, including fractals, do not have integer Hausdorff dimensions. Due to the significant technical advances made by Abram Samoilovitch Besicovitch, allowing the calculation of dimensions for highly irregular or "rough" sets, this dimension is also commonly known as the Hausdorff-Besicovitch dimension [13].

The fractal dimension, a measure characterizing the geometric and topological complexity of fractal sets, is often defined using the Hausdorff-Besicovitch dimension. While there are various ways to define the fractal dimension, one of the most common is precisely the Hausdorff-Besicovitch dimension. The most popular method today for calculating the fractal dimension is the box-counting method. This method involves counting the number of boxes $N(\epsilon)$ of size ϵ needed to cover the entire object in the image. As the value of ϵ increases, the number of boxes needed to cover the object decreases. The fractal dimension is obtained by calculating the slope of the best-fit line from a graph of $\log(N(\epsilon))$ against $\log(1/\epsilon)$ [14].

The Hausdorff-Besicovitch dimension (D) is defined for fractal sets F as follows

$$D = \frac{\text{Log}(N(\epsilon))}{\log(1/\epsilon)} \quad (1)$$

Where:

D: is the Fractal dimension

$N(\epsilon)$: Is the minimum number of assemblies (ϵ -cover) required to completely cover fractal assembly F with elements of diameter not greater than ϵ .

ϵ : This is the size of the element of the ϵ -cover.

In simpler terms, the fractal dimension provides valuable information about the variation in the number of smaller sets needed to cover a fractal set as the size of the covering elements is adjusted. When applied to the analysis of medical images, this methodology has proven its utility in various disciplines, from the detailed examination of coronary branching to the comprehensive assessment of neurodegenerative diseases and dementia through ultrasound images. These advances, guided by key dates and notable achievements, have transformed the understanding and application of the fractal dimension in various scientific fields [15] [16] [17].

2. Methodology

This study adopted an observational approach based on a series of cases, utilizing data from the LiTS - Liver Tumor Segmentation Challenge (LiTS17) and the CHAOS - Combined (CT-MR) Healthy Abdominal Organ Segmentation dataset. It included 130 computed tomography's from pathological patients, with their corresponding liver-segmenting masks, obtained from LiTS17, and 40 computed tomography's from healthy patients, with 20 volumes of masks from CHAOS. To address the diversity of medical formats, the versatile capabilities of Python were employed [18], implementing custom instructions for the efficient reading of medical volumes with variable formats and procedures.

The datasets were provided in .nii and DICOM formats, and to ensure equality in the number of patients in both populations, 20 volumes were selected from the first dataset. Subsequently, slices were extracted from each volume and exported to JPG image files (Figure 1). This approach allowed for the standardization of data, facilitating consistent comparison and analysis across both patient groups.

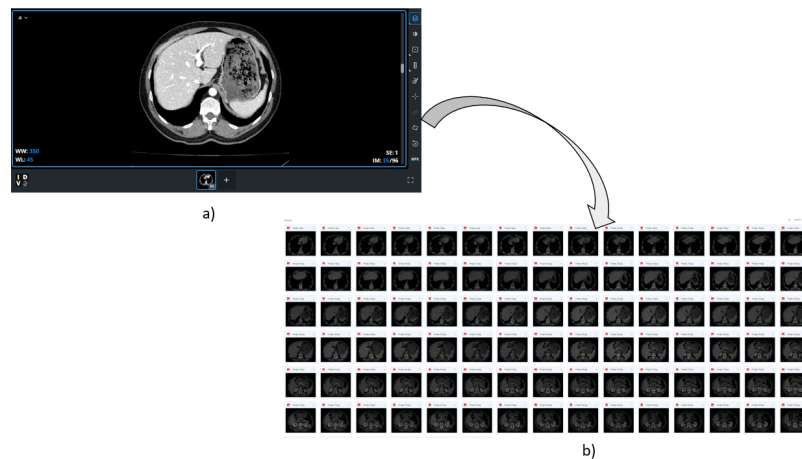


Figure 1: Extracting the slices from the .nii and DICOM files and exporting them as a JPG image. In the subsequent phase, we utilized this set of images as input for a liver segmentation process. This procedure involves integrating information from the medical images with the pre-existing mask, thus generating a detailed and accurate mapping of hepatic regions in each image. Leveraging the richness of data provided by the original images and guided by the pre-existing mask in the selected image set, this process enables a more suitable and detailed delineation of the hepatic structure (Figure 2, section b) in the data from each slice extracted from both groups of tomographic volumes (Figure 2, section a). The result can be observed in section c of Figure 2.

After this process, we proceed to create a copy of the original image. Subsequently, we identify the coordinates where the liver mask has white values, indicating specific areas of interest. Next, we replace the pixels at these coordinates in the mask with the corresponding pixels from the original image. This procedure essentially involves overlaying and merging the information contained in the mask with the visual information from the original tomography. The obtained result is an effective segmentation of the organ, where all its anatomical and structural characteristics captured by the tomography are accurately represented.

This approach of integrating the mask and the original image serves as a robust method to precisely highlight and delineate hepatic regions (Figure 2, section d). The procedure is based on the binary nature of a mask, where pixels are classified into two distinct categories: 0, representing the background or areas to be omitted, and 1, indicating the foreground or areas of interest. By assigning these values, we precisely establish which regions of the original image should be preserved (in the case of the mask with a value of 1) and which should be suppressed or excluded (when the mask has a value of 0). This approach proves to be an efficient method to accurately highlight and isolate anatomical structures of interest.

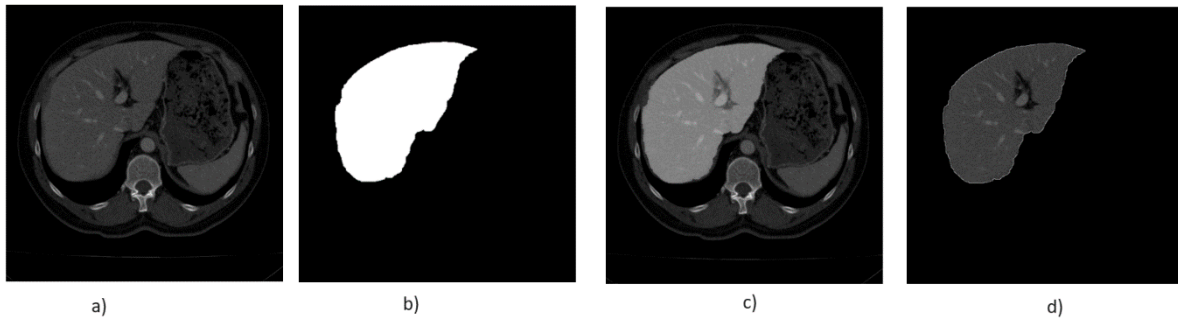


Figure 2: Masking and Pixel Replacement Process for Liver Segmentation on the Original Image.

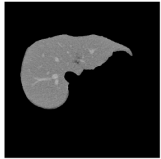
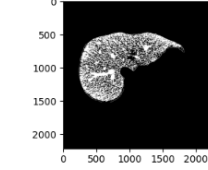
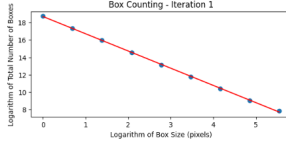
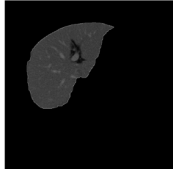
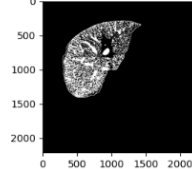
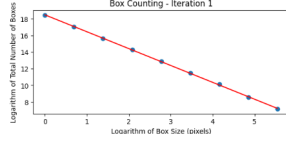
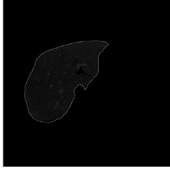
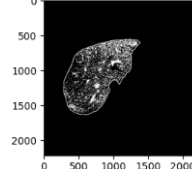
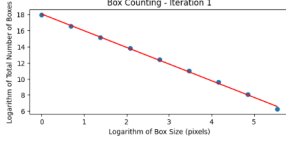
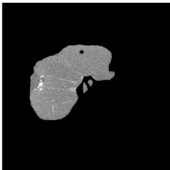
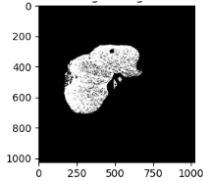
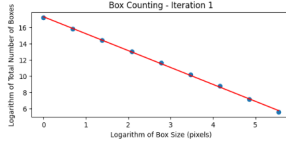
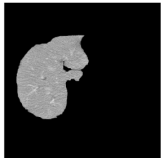
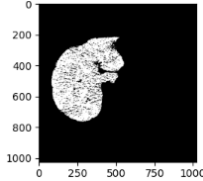
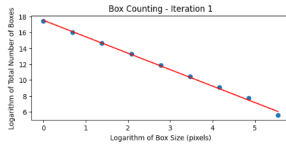
With the set of JPG images from each group, we performed the mathematical analysis of the fractal dimension. In this process, the first step involves scanning the pixels and calculating the mean to use as a threshold in the transformation from original to binary images. The binarization threshold is crucial because pixels are classified into two categories: those belonging to the object of interest and those that do not (Table 1, column 2). As a second step, the fractal dimension is calculated on that binarized image, and each dimension is stored in a list for each group of images.

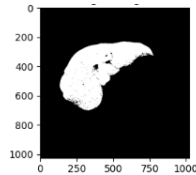
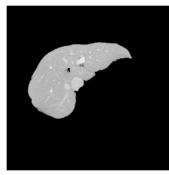
The algorithm we used to compute the fractal dimension is the following.

1. Initialization:
 - Start with a binary image representing the fractal set. In this case, the image is a matrix of zeros and ones, where ones indicate the presence of the fractal set, and zeros indicate its absence.
2. Initial Box Size Definition (ϵ):
 - Choose an initial box size, denoted as ϵ (epsilon). This size determines the size of the square boxes that will be used to cover the image.
3. Box Creation:
 - Create a matrix of square boxes, where the value at each position indicates whether the box covers the fractal set or not. Initially, for this research, start with the pixel size of the image (512) (Table 1).
4. Fractal Set Coverage:
 - Overlay the boxes on the fractal set image. Each box that matches the fractal set is marked as "1" in the box matrix (Figure 3).
5. Box Counting:
 - Count the number of boxes that have at least one pixel inside the fractal set. This number is the result of box counting for the current box size (Table 1).
6. Box Size Reduction (ϵ):
 - Reduce the box size (ϵ) by half and repeat steps 3-5 for the new box size (Figure 3).
7. Iteration:
 - Repeat the process for different box sizes, usually halving in each iteration, until the box size is as small as desired; in this research, the smallest size is one pixel.

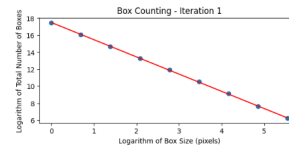
8. Result Recording:
 - Record the number of boxes needed to cover the fractal set for each box size (Table 1).
9. Logarithmic Analysis:
 - To analyze the relationship between box size and the number of boxes needed, take the logarithm of both sides. This is done to visualize the relationship on a logarithmic scale (Table 1).
10. Result Visualization:
 - Visualize the results graphically, often using a log-log plot where the x-axis represents the logarithm of the box size, and the y-axis represents the logarithm of the number of boxes needed (Figure 3).
11. Fractal Dimension Estimation:
 - The slope of the line in the log-log plot provides an estimate of the fractal dimension of the set.

Table 1.
Box-Counting for 6 patients with a box size of one pixel (minimum possible).

Original Image	Binarized image	Patient	Box-Counting Chart	FD
		Non-pathological		1.562
		Non-pathological		1.560
		Non-pathological		1.547
		Pathological		1.456
		Pathological		1.487



Pathological



1.200

In Table 1, we can see the binarization of images from some patients, both pathological and non-pathological. The Box-Counting Chart shows the log-log plot of box counting. Each point on the graph represents the box size (on the x-axis) and the total number of boxes needed to cover the image (on the y-axis). In this way, we can observe a more homogeneous structure in terms of binarization in non-pathological patients. The above observation validates that the lower complexity of the fractal dimension in images of pathological patients (Table 1) may be related to metabolic alterations that would be indirectly observed using the weighted pixel intensity threshold. This could provide a pathway for in-depth analysis in future projects. A healthy liver tends to show a uniform and efficient distribution of contrasts, while in a liver affected by cancer, changes in blood flow could result in noticeable alterations in the uptake and dispersion of contrast, influencing the interpretation of medical images, such as tomography (Figures 3 and 4) [19].

With the stored fractal dimensions, we filter out any slice that represents an image with completely black pixels, i.e., slices from the tomography where the liver is not present, mainly the first and last slices of the study. It is this reduced filtered list to which the distribution study and the non-parametric test of mean difference (Mann-Whitney U) were applied.

3. Results.

In the following table (Table 2), we can see the summarized analysis of the images, including the selection of slices that underwent fractal dimension calculation. A total of 20 tomography volumes were processed for each patient group, ensuring a representative sample from both sets. The segmentation of the tomography slices resulted in a significant number, initially extracting 11,437 for pathological patients and 2,874 for non-pathological ones. This was derived from the size of the slices used as configuration in the tomographic equipment. For the research, those slices without the presence of the hepatic organ were eliminated, meaning the masks that showed a completely black image, leaving us with a final number of images of 3,412 for pathological patients and 2,289 for non-pathological ones. Analyzing this group of images, we obtained a mean DF of 1.36 in "Non-pathological Patients," while in "Pathological Patients," it was slightly lower, with a mean of 1.25. In the following table (Table 2), we can see the summarized analysis of the images, including the selection of slices that underwent fractal dimension calculation.

Table 2.
Data from the study.

Study Group	Volumes of Analyzed Tomography	Extracted slices	Cuts without organ to be segmented	Segmented organ cuts	Average DF	Median DF
Non-pathological	20	2874	585	2289	1.36	1.41
Pathological	20	11437	8025	3412	1.25	1.32

Now, these differences in populations alone are not sufficient for the classification of pathological and non-pathological patients, as seen in Figure 6 where there is a significant intersection between results for both cases (pathological and healthy). However, fractal dimension can be integrated with other clinical features and biomarkers to improve the robustness of classification models. This could result in more comprehensive and accurate systems to distinguish between patients with pathological and non-pathological livers, as texture is the most appropriate descriptor for mass detection in images [20].

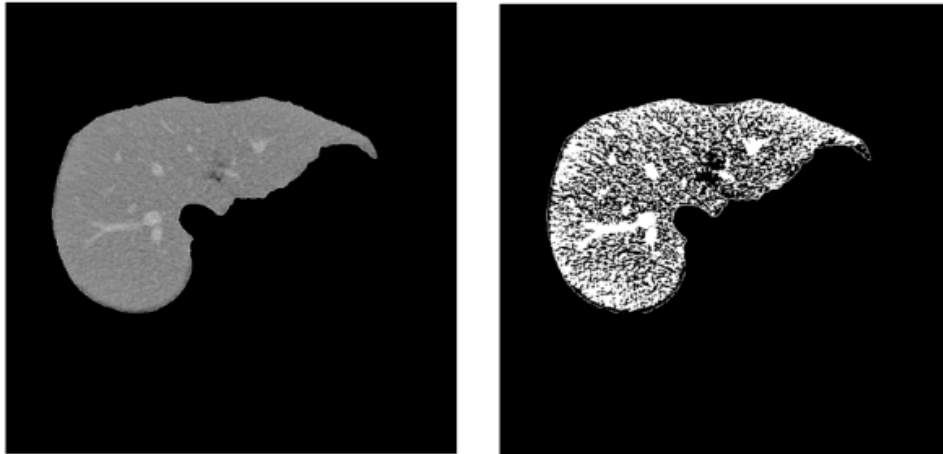


Figure 3: In the left side non-pathological image of the patient's liver, in the right side treated using weighted pixel intensity threshold.

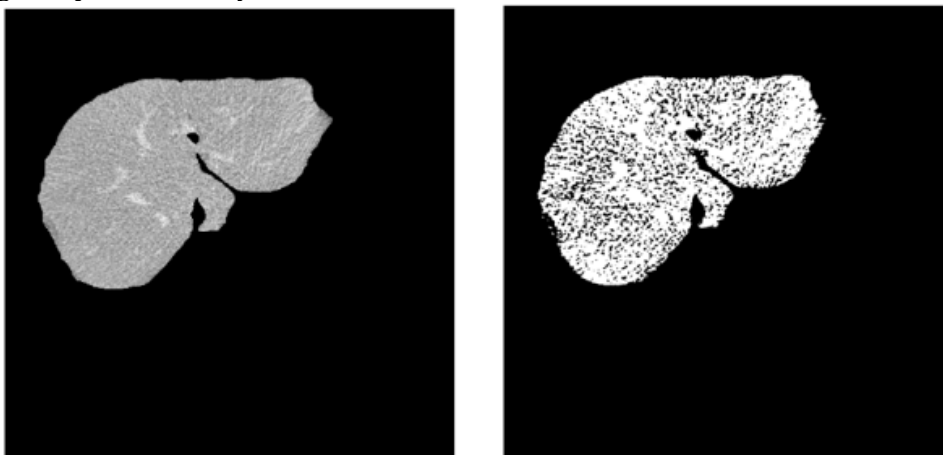


Figure 4: in the left side pathological image of the patient's liver, in the right side treated using weighted threshold of pixel intensity.

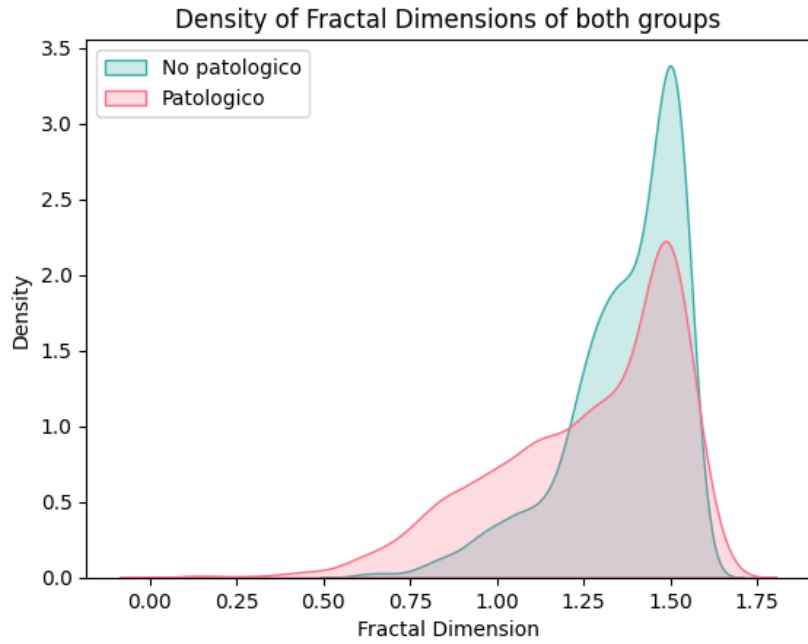


Figure 5: Density of the distribution of the study populations.

In the previous graph (Figure5), the Y-axis shows the occurrence density of fractal dimension values, indicating the concentration of values in both study groups and providing a general idea of how they are distributed in amplitude, a part that shows differences in the studied groups.

In the follow Figure (Figure 6), we can observe a relative distance between the means and medians of the studied data, leading us to theorize that by using fractal dimension as a variable for classification models, a quantitative evaluation of tomographic images could be carried out. This would allow for a more precise characterization of the complexity and irregularity of hepatic structures, providing valuable information for diagnosis and treatment. By quantifying fractal complexity over time in images and even at the cellular level, doctors could gain insights into the evolution of pathology and adjust treatment strategies [21] [22]

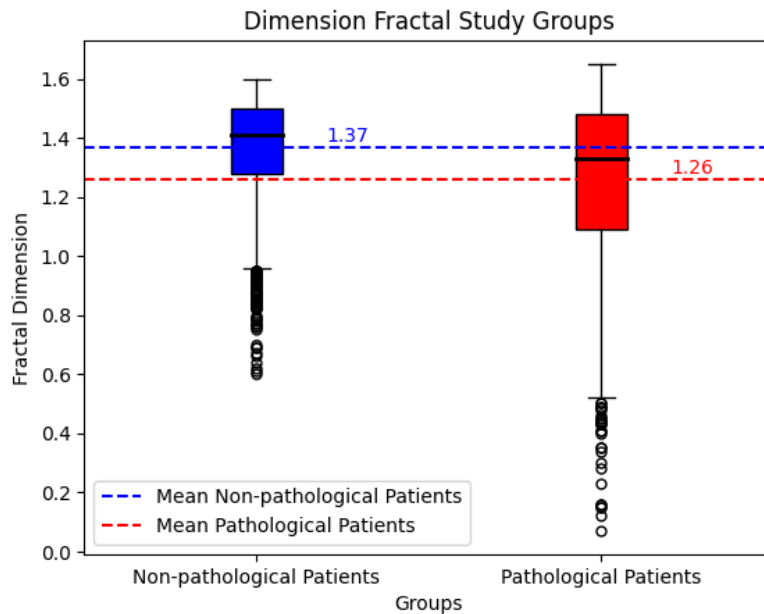


Figure 6: Box-plot of the study populations.

The above graph (Figure 6) provides a clear insight into the behavior of fractal dimensions in the analyzed patients. The X-axis contains the studied groups, while the Y-axis represents the values of the fractal dimension, here is where we can observe the variability of fractal dimensions among the groups and how they behave along this axis. The interquartile range (IQR) can be observed in the height of the boxes, and, in turn, the whiskers extending from the boxes upward and downward represent the dispersion of data outside the interquartile range, highlighting outliers, indicated as points outside the whiskers. Meanwhile, horizontal lines inside the boxes represent the medians presented in Table 2, which are slightly distant from each other. Additionally, a new feature is the horizontal lines outside the boxes; these dashed lines represent the mean (Table 2) of the data in each group, allowing for a comparison of the mean and median in each dataset.

Mann-Whitney U Test

U-Test Statistic: 4701167.0

p-value: 4.965716675822758e-39

With this result, we conclude that there is a significant difference between the populations, suggesting a contribution of this information derived from the fractal analysis of images in the future generation of useful models in the classification of hepatic neoplasms.

4. Conclusions.

This study presents relevant evidence concerning the description of liver texture and characteristics, which carries significant implications for the diagnosis and classification of liver diseases, particularly in the context of cancer. Through the application of an innovative approach utilizing pixel intensity weighting in medical images, precise segmentation of hepatic regions has been achieved. Empirical evidence has shown that this methodology is highly useful, as it has successfully revealed significant differences in fractal dimension between patients with and without liver pathologies. Considering the complex nature of hepatocarcinogenesis, the observed variation in pixel segmentation among these groups suggests the possibility that liver lesions may exhibit diverse blood flow patterns, thus influencing the absorption and distribution of contrast agents in imaging studies. Pathological patients demonstrate visually smoothed regions in their images, indicating that a less complex pixel-level structure is being analyzed, as illustrated in Table 1.

The findings of this study provide an informative basis for future research endeavors, such as collaboration with specialists to improve segmentation techniques and to undertake more diverse computational analyses. In addition to advancing clinical understanding, the image dataset generated from this study, which includes the segmented organ with its corresponding original image extracted from the tomographic volume, holds tremendous potential in serving as a foundation for further investigations. This dataset can facilitate more advanced analyses that take into consideration fractal features, weighted thresholds, and clinical data, potentially leading to enhanced models for the classification of liver pathologies.

References.

- [1] D. Mashaal, A. A. Melin, Jeffrey Douaiher, J. Douaiher, C. Lin, . W. K. Zhen, S. M. Hussain , J.-F. H Geschwind,. M. B. Majella Doyle, G. K. Abou-Alfa y C. Are, «A Review and Update of Treatment Options and Controversies in the Management of Hepatocellular Carcinoma,» *Annals of surgery*, (2016) 1112-25. doi: 10.1097/SLA.0000000000001556
- [2] WHO, "World Health Organization",» 2022, https://www.who.int/es/health-topics/cancer#tab=tab_1.

- [3] R. Chaiteerakij, B. D. Addissie y L. R. Roberts, «Update on biomarkers of hepatocellular carcinoma,» *Clinical Gastroenterology and Hepatology*, (2015) . 237-45, 2015. doi: 10.1016/j.cgh.2013.10.038
- [4] A. P. Pérez, «Ultrasound and liver, *Family Medicine. SEMERGEN*, (2003), 78-97. 2003. doi: 10.1016/S1138-3593(03)74163-X
- [5] E. J. F. Morales, S. A. M. Zuñiga, P. A. A. Acuña y D. G. G. Méndez, «Comparison of diagnostic accuracy of computed tomography and magnetic resonance imaging of liver lesions,» *RECIAMUC*, (2023). doi: 10.26820/reciamuc/7.(2).abril.2023.517-524
- [6] J. L. Montes de Oca Mastrapa, A. Cisneros Carmenate y J. Pérez Betancourt, «Giant hepatocellular carcinoma in cirrhotic liver. Case Presentation and Literature Review,» *Finlay Journal*, (2022), URL: <https://revfinlay.sld.cu/index.php/finlay/article/view/1049>.
- [7] A. S. Graua, I. V. López, N. D. Rodríguez y J. S. Cabra, «Hepatic ultrasound: focal lesions and diffuse diseases,» *Family Medicine. SEMERGEN*, (2016). doi: 10.1016/j.semerg.2014.10.012.
- [8] G. Fonte, M. Emma, M. Misas Menéndez y I. González Santana, «Clinical, imaging and pathological characterization of focal liver lesions,» *MediSur*, (2014) URL: <https://medisur.sld.cu/index.php/medisur/article/view/2711>.
- [9] J. Illescas-Cárdenas, P. Rodríguez-Nava y E. Dena-Espinoza, «Evaluation of liver lesions by multiphase multislice tomography: structured report proposal.» *Anales de Radiología México*.(2017). URL: https://www.analesderadiologiamexico.com/previos/ARM%202017%20Vol.%2016/ARM_17_16_2_Abril-Junio/arm_17_16_2_087-101.pdf
- [10] D. P. Granda, «Hepatic space-occupying lesions in Magnetic Resonance Imaging: a daily challenge for the radiologist,» *Revista Argentina de Diagnóstico por Imágenes*, (2016) 44-56, doi: 10.13140/RG.2.2.30812.54409 .
- [11] M. d. C. MT y C. JD, «Carcinogenesis, » *Public Health in Mexico*,» *salud pública de méxico* , (2011). URL: <https://www.scielo.org.mx/pdf/spm/v53n5/a08v53n5.pdf>
- [12] N. Plant, «Can systems toxicology identify common biomarkers of non-genotoxic carcinogenesis?,» *Toxicology*, (2008), 164-9, doi: 10.1016/j.tox.2008.07.001
- [13] Dhama K, Latheef SK, Dadar M, Samad HA, Munjal A, Khandia R, Karthik K, Tiwari R, Yattoo MI, Bhatt P, Chakraborty S, Singh KP, Iqbal HMN, Chaicumpa W, Joshi SK, «Biomarkers in Stress Related Diseases/Disorders: Diagnostic, Prognostic, and Therapeutic Values,» *Front Mol Biosci.*, (2019), doi: 10.3389/fmolb.2019.00091.
- [14] T. Gneiting, H. Ševčíková y D. B. Percival, «Estimators of Fractal Dimension: Assessing the Roughness of Time Series and Spatial Data,» *Statistical Science*, (2016), vol. 27, no. 2, 247-277. URL: <http://www.jstor.org/stable/41714797>.
- [15] M. Luppe, «Fractal dimension based on Minkowski-Bouligand method using exponential dilations,» *Electronics Letters*, (2015),475-477, doi: 10.1049/el.2015.0156.
- [16] Rodríguez-Velásquez, Javier O, Prieto, Signed E, Ortiz, Liliana, Ronderos, Miguel, & Correa, Catalina. (2010). Mathematical diagnosis of pediatric echocardiography with fractal dimension measurements evaluated with intrinsic mathematical harmony. *Colombian Journal of Cardiology*, pp. 79-86. URL: http://www.scielo.org.co/scielo.php?script=sci_arttext&pid=S0120-56332010000200007&lng=en&tlng=es.
- [17] Elina T. Ziukelis, Elijah Mak, Maria-Eleni Dounavi, Li Su, John T O'Brien, Fractal dimension of the brain in neurodegenerative disease and dementia: A systematic review, *Ageing Research Reviews*, (2022),doi.org/10.1016/j.arr.2022.101651.
- [18] Forero, W., & Ochoa, C. O. (2017). Fuzzy logic elements and morphological operators applied to the filter of medical images, *Memories of the geometry meeting and its applications*, pp. 81-86, URL: <http://funes.uniandes.edu.co/12861/1/Forero2017Elementos.pdf>

- [19] P.E. Cossio-Torricoa, C.R. Ramírez-Carmonab, M. Stoopen-Romettic, A. Perochena-González, L.A. Sosa-Lozanod, E. Kimura-Hayama, (2015), Liver-specific gadoxetic acid-enhanced magnetic resonance for focal lesion evaluation, *Journal of Gastroenterology of Mexico*, pp. 267-275, doi: 10.1016/j.rgmx.2015.06.011
- [20] Zebari, D.A.; Ibrahim, D.A.; Zeebaree, D.Q.; Mohammed, M.A.; Haron, H.; Zebari, N.A.; Damaševičius, R.; Maskeliūnas, R. Breast Cancer Detection Using Mammogram Images with Improved Multi-Fractal Dimension Approach and Feature Fusion. *Appl. Sci.* 2021, 11, 12122. <https://doi.org/10.3390/app112412122>
- [21] Elkington, L.; Adhikari, P.; Pradhan, P. Fractal Dimension Analysis to Detect the Progress of Cancer Using Transmission Optical Microscopy. *Biophysica* 2022, 2, 59-69. <https://doi.org/10.3390/biophysica2010005>
- [22] Pala, MA, Çimen, ME, Akgül, A. et al. Fractal dimension-based feasibility analysis of cancer cell lines in lensless holographic microscopy using machine learning. *EUR. Physics. J. Specifications. Up.* 231 , 1023–1034 (2022). <https://doi.org/10.1140/epjs/s11734-021-00342-3>